A strongly fluctuating quasi-two-dimensional insulator (invited)

C. Broholm, G. Aeppli, G. P. Espinosa, and A. S. Cooper
AT&T Bell Laboratories, Murray Hill, New Jersey 07974

We describe neutron-scattering data for $SrCr_{8-x}Ga_{4+x}O_{19}$, a layered compound containing planes of $S = 3/2$ Cr^{3+} ions which form Kagomé lattices. Despite strong antiferromagnetic interactions ($\theta_{CW} \approx -500$ K), fluctuations account for more than 75% of the free ion moment at 1.5 K. The spectrum (averaged over reciprocal space) is gapless and resembles that of a 2D long-range-ordered antiferromagnet, as does the low-temperature specific heat of the compound. Even so, the static correlation length does not exceed 7 ± 2 Å. Monte-Carlo simulations of the antiferromagnetic three-state Potts model on the Kagomé lattice show that this model does not have a finite temperature phase-transition. Even at $T = 0$, there does not seem to be true long-range antiferromagnetic-order. However, the magnetic correlations decay algebraically rather than exponentially. The implications of this result for the ground-state of $SrCr_{8-x}Ga_{4+x}O_{19}$ is discussed.

I. INTRODUCTION

Closely related to the absence of conventional long-range magnetic order in one dimension is the occurrence of quantum effects, most notably the Haldane gap. Apart from low dimensionality, also disorder, nonmagnetic dilution and geometrical frustration suppress the development of long-range order. Whereas the former two mechanisms often lead to spin-freezing and rather classical properties, geometrically frustrated antiferromagnets (AFM) may present interesting analogies to the 1D spin liquid.

Recently, Obradors *et al.*[1] discovered a spinel-related insulator $SrCr_{8-x}Ga_{4+x}O_{19}$ [SCGO(x)] with an extreme degree of magnetic frustration. The magnetic properties of this compound are due to AFM coupled Cr^{3+} ions which, surrounded by weakly distorted oxygen octrahedra, are good realizations of $S = 3/2$ Heisenberg spins. Obradors *et al.* showed that despite a Curie–Weiss temperature $\theta_{CW} = -492$ K, long-range magnetic order does not occur to the lowest temperature (4.2 K) investigated. Ramirez *et al.*[2] discovered spin glass transitions in SCGO(x) at x-dependent temperatures T_g^{dc} between 3.5 and 7 K. They also suggested that the geometrical frustration in this material arises from layers of Cr^{3+} arranged in Kagomé lattices. Figure 1(a) shows the Cr^{3+} sites in SCGO(x)[1] which form a stack of dense Kagomé (labeled $12k$) lattices separated by more dilute triangular lattices ($2a$ and $4f$).

The Kagomé lattice [see Fig. 1(b)] can be viewed as a triangular lattice with lattice parameter $a/2$ with vacancies at the sites of a triangular superlattice with lattice parameter a. The AFM Ising model on the Kagomé lattice has been studied analytically[3] and it has been proven that there is no phase-transition even at $T = 0$, where the correlation length remains finite, $\xi = 1.7a$, and the entropy large $S = 0.7239 \cdot R \ln 2$. The ground state for quantum spins is of great current interest. Elser[4] has considered the $S = 1/2$ AFM on the Kagomé lattice in the context of nuclear magnetism in ^{3}He films, and predicted a phase transition from a spin liquid of singlets to a valence bond solid. Ritchie *et al.*[5] and Chandra and Coleman[6] describe the ground state as a spin nematic with long-range order not in the staggered magnetization but in the so-called twist.

In this paper we describe neutron-scattering data from SCGO(x) which establish that the correlations in this compound are two-dimensional, very short ranged ($\xi \approx 7$ Å), and with local order which corresponds to tripartition of the Kagomé lattice. Our data are consistent with spin-freezing for $T < T_g^{dc} = 5$ K but 75% of the net moment remains fluctuating to the lowest temperatures, thus precluding a description in terms of a conventional spin glass. Also the local magnetic fluctuation spectrum resembles that of a long-range ordered two-dimensional Heisenberg AFM. We furthermore show by Monte-Carlo simulation on the Kagomé lattice that the three-state Potts model, which is closely related to vector spin models, does not have a finite-temperature phase transition, but displays algebraically decaying AFM correlations with the same local order as we find in SCGO(x).

II. SAMPLE AND EXPERIMENTAL TECHNIQUE

The sample used in this experiment was 50 g of powder made by cooling $SrCrO_3$, Cr_2O_3, and Ga_2O_3 in a SrO-B_2O_3 solvent. The neutron powder diffraction at 1.5 K could be indexed by the hexagonal structure previously reported[1] with lattice parameters $a = 5.80$ Å and $c = 22.7$ Å. Susceptibility measurements in the Curie–Weiss regime showed that the Cr concentration in our sample was 11% less than in ceramic SCGO(0) samples produced by solid-state reaction.[7] Since even the $x = 0$ samples have partial occupancy of Ga on Cr sites[1] it is reasonable to assume that the Cr deficiency in our sample arises from further substitution of nonmagnetic Ga for Cr. Assuming that the Cr concentration on sites of different symmetry is reduced by the same fraction, the Cr occupancy of the $12k$, (Kagomé), $2a$, and $4f$ layers is 80%, 90%, and 80%, respectively. The Cr concentration in all layers is above the 2D

 0021-8979/91/084968-06$03.00

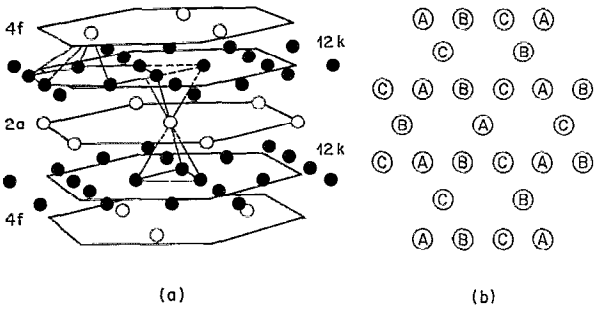

FIG. 1. (a) Location of Cr atoms (filled and open circles) in SCGO(x). 12 K layers containing filled circles are Kagomé planes. (b) Kagomé lattice. A, B, and C indicate sublattices in the periodic tripartition of the lattice. (From Ref. 8.)

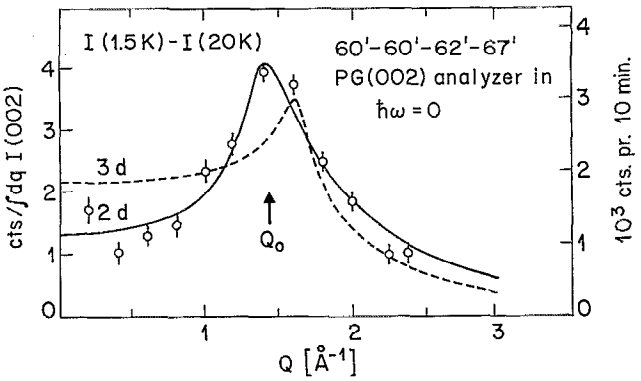

FIG. 2. Difference between elastic scattering at $T = 1.5$ K $\ll T_g$ and $T = 20$ K $\gg T_g$. Data from configuration No. 1 (see Table I for details of configurations). (After Ref. 8.)

percolation threshold so that in a naive sense, dilution does not limit the correlation length.

The neutron-scattering experiments were performed using the TAS-1 triple-axis spectrometer in the DR-3 reactor at Risϕ National Laboratory in Denmark. Cold neutrons were monochromated and vertically focused on the sample by pyrolytic graphite crystals set for their (002) Bragg reflection [PG(002)]. Be or PG filters were used to remove λ/n components of the incident beam. The scattered neutrons were analyzed for scattering angle and energy distribution by a flat PG(002) crystal. The energy transfer to the sample $\hbar\omega = E_i - E_f$ was varied by changing the final energy, E_f, at a fixed incident energy E_i.

We normalize inelastic scattering data taken with different configurations to $A(002)\Delta$ where $A(002)$ is the Q-integrated intensity of the (002) Bragg peak of SCGO(x) and Δ is the full width at half maximum (FWHM) of the incoherent energy resolution. Furthermore, inelastic data from each configuration were corrected by an $\hbar\omega$-dependent factor to take into account the dependence of the analyzer transmission on the varying final energy, E_f. Elastic scattering was normalized to $A(002)$. Table I summarizes the different configurations used.

III. STATIC SPIN-CORRELATIONS

In agreement with previous neutron-scattering experiments on SCGO(0), no magnetic Bragg peaks develop in our sample down to the lowest temperature (1.5 K) accessed. However, the difference between field-cooled and zero-field-cooled dc susceptibility below T_g in SCGO(x) indicate that static or quasi-static spin-correlations are present at low temperatures. Such correlations give rise to elastic magnetic scattering. In search of these, we measured the difference between elastic scattering at 1.5 K $\ll T_g$ and 20 K $\gg T_g$. The result is shown as a function of momentum transfer, Q, in Fig. 2. Rather than being confined to sharp Bragg peaks, the elastic scattering forms a broad peak extending over the full range of Q accessed. Thus, the static correlations which develop have only very short range. To extract more specific information we must take into account that the scattering from a powder sample is proportional to the spherically averaged two-spin correlation function. The dashed line in Fig. 2 is a spherically averaged three-dimensional Lorentzian which would be relevant if the correlations were isotropic. This function does not account well for the data. If we instead assume that the short range order is two dimensional, corresponding to rods of scattering parallel to the c axis and confined according to a two-dimensional Lorentzian around a characteristic $\mathbf{q}_0$ in the basal plane, the spherically averaged cross section (solid line) yields a satisfactory agreement between model and data. In both calculations we have taken the spins to be isotropically polarized as is appropriate for Heisenberg $S = 3/2$ spins. Since the distance between spins within Kagomé planes is close to that between spins displaced along the c axis [Fig. 1(a)], it is not obvious that magnetic correlations in this material should be two dimensional. The effective two dimensionality may be the result of the three times lower Cr^{3+} concentration in the triangular lattice planes which separate Kagomé planes and the frustration of interactions between spins occupying different planes. From the best fit to the data we extract a two-dimensional correlation length $\xi = 7 \pm 2$ Å corresponding to just twice the nearest neighbor separation in the Kagomé plane. We also deduce the wave vector for the short range order: $|\mathbf{q}_0| = 1.4 \pm 0.1$ Å^{-1}. If the correlations exist only in the Kagomé planes of SCGO(x), $\mathbf{q}_0$ itself must lie in the basal plane and should correspond to a high symmetry point in the hexagonal reciprocal lattice with lattice parameter $a^* = 4\pi/\sqrt{3}a = 1.25$ Å^{-1}. The modulus $|\mathbf{q}_0|$ is indeed indistinguishable from $(\frac{2}{3}\,\frac{2}{3})$ the fundamental wave vector of the $\sqrt{3}\times\sqrt{3}$ superlattice inherited

TABLE I. Configurations used with corresponding peak and Q-integrated intensity of (002) and energy resolution.

Conf. No.	E_i meV	Collimation minutes	$I(002)$ cts s^{-1}	$A(002)$ Å^{-1} cts s^{-1}	Δ meV
1	5	60'-60'-62'-67'	48	1.41	0.2
2	3.6	60'-30'-28'-67'	10	0.15	0.1
3	13.9	60'-60'-62'-104'	79	4.9	1.2

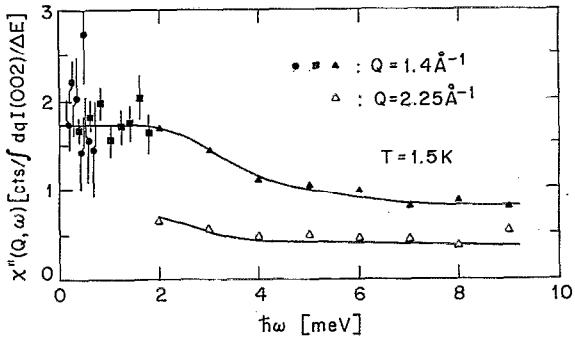

FIG. 3. $\hbar\omega$ dependence of $\chi''(Q,\omega)$ at $T = 1.5$ K, $Q = 1.4$ Å, and $Q = 2.25$ Å derived from inelastic magnetic neutron scattering. ■ and □ are from configuration No. 1, ● from configuration No. 2, and ▲ and △ from configuration No. 3.

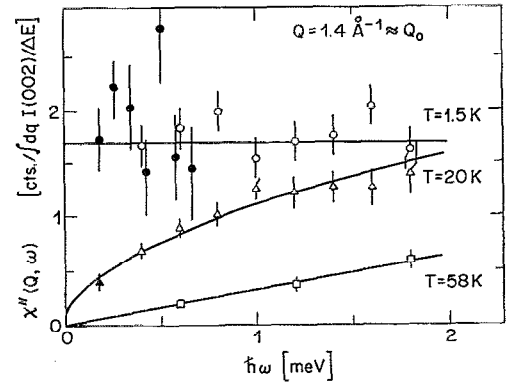

FIG. 4. $\chi''(Q_0,\omega)$ for $\hbar\omega \leq 2$ meV at three temperatures. Solid lines represent best fits to Eq. (5). Open symbols are from configuration No. 1, filled symbols configuration No. 2. (From Ref. 8.)

by the Kagomé lattice from its (xy) magnetically ordered triangular lattice parent [see Fig. 1(b)].

IV. MAGNETIC FLUCTUATIONS AT $T \ll T_g$

In a previous publication[8] we have shown that the Q-dependence of the inelastic magnetic scattering is quite similar to that of the elastic scattering of Fig. 2 for energy transfer $\hbar\omega \lesssim 8$ meV. This result confirms expectations, based on the large negative Curie–Weiss temperature, that the energy scale of the interactions giving rise to the AFM correlations is well above 8 meV. Figure 3 shows $\chi''(Q,\omega)$ vs $\hbar\omega$ at $Q = 1.4$ Å$^{-1} = |\mathbf{q}_0|$. The spectrum was derived via the fluctuation-dissipation theorem[9] from constant-Q scans which measure $S(Q,\omega)$. To interpret these data, note that for $|\hbar\omega| \lesssim 8$ meV it is a good approximation for our powder sample to express $\chi''(Q,\omega)$ as $\chi''(Q,\omega) \propto C(Q)\chi''(\omega)$ where $\chi''(\omega) = \int \mathbf{dq}\chi''(\mathbf{q},\omega)$. The data of Fig. 3 are thus a measure of the ω dependence of the $\mathbf{q}$ averaged, or local, response function, $\chi''(\omega)$. Thus, $\chi''(\omega)$ is a monotonically decreasing function up to 8 meV, the only identifiable energy scale being around $\hbar\omega^* \approx 3$ meV where the decrease is steepest. It is interesting that whereas $k_B T_g = 0.4$ meV $\ll \hbar\omega^*$ and $k_B|\theta_{CW}| = 37$ meV $\gg \hbar\omega^*$, $\hbar c/\xi = 5$ meV, where c is the velocity one may derive from the limiting T^2 dependence of the specific heat,[2,7] is of the same order as $\hbar\omega^*$. If propagating excitations involving a hidden, but ordered degree of freedom exist in SCGO(x), it is conceivable that the frequency of the excitations with wavelengths of order ξ would define a characteristic energy for $\chi''(\omega)$.

Our neutron-scattering data provide a rigorous measure of the relative amount of frozen and fluctuating moment. The $\mathbf{q}$ integrated magnetic neutron scattering cross section is proportional to

$$S(\omega) = \int \mathbf{dq} S(\mathbf{q},\omega) = \frac{1}{2\pi\hbar}\int dt \sum_l \langle S_l(0)S_l(t)\rangle \exp(i\omega t). \quad (1)$$

In a powder sample, spherical averaging has already taken place[9] so $S(\omega) \propto \int dQ\, S(Q,\omega)$. The Q-integrated nominally elastic magnetic powder scattering measured with the energy-resolution function $R(\hbar\omega/\Delta)$ is

$$N\langle\mu^2\rangle|_{|\hbar\omega|<\Delta} = \int_{-\infty}^{+\infty} d\omega R(\hbar\omega/\Delta) S(\omega). \quad (2)$$

Since

$$\lim_{\Delta\to 0^+} \langle\mu^2\rangle|_{|\hbar\omega|<\Delta} = (1/N) \sum_l \lim_{t\to\infty} \langle S_l(0)S_l(t)\rangle$$

we can interpret $\langle\mu^2\rangle|_{|\hbar\omega|} < \Delta$ as the mean square moment frozen on the time-scale $t = 2\pi\hbar/\Delta$ given by the energy resolution of the experiment. Analogously

$$N\langle\mu^2\rangle|_{\hbar\omega>\Delta} = \int_{|\hbar\omega|>\Delta} d\omega S(\omega) \quad (3)$$

is the mean squared moment fluctuating at frequencies $|\hbar\omega| > \Delta$. Combining normalized elastic and inelastic constant $\hbar\omega$ and constant Q scans for $\hbar\omega < 8$ meV we obtain

$$\epsilon(\Delta = 0.2 \text{ meV}) = \frac{\langle\mu^2\rangle_{|\hbar\omega|>\Delta}}{\langle\mu^2\rangle_{|\hbar\omega|<\Delta}} > 4. \quad (4)$$

Ground-state quantum fluctuations thus account for more than 75% of the squared free ion moment in SCGO(x). In fact, our data are consistent with $\lim_{\Delta\to 0}\epsilon(\Delta) = \infty$ which would imply a spin-liquid ground state for SCGO(x). However, the presence of hysteresis in dc susceptibility data[2] probably excludes this scenario.

The low-energy limit of $\chi''(\omega)$ is of special interest because it is related to the $T\to 0$ limit of the magnetic contribution to thermodynamic properties. Figure 4 shows $\chi''(\omega)$ for $\hbar\omega < 2$ meV at three temperatures. Focusing first on the data at $T = 1.5$ K $\ll T_g$, we note that there is no evidence of a gap in the excitation spectrum down to $\hbar\omega = 0.15$ meV. This result, which is consistent with the absence of exponential behavior in thermodynamic properties below T_g, indicates that as expected for Heisenberg or xy spins, there is no anisotropy gap in the magnetic excitation spectrum. More surprising is that at 1.5 K, $\chi''(\omega)$ is indistinguishable from constant for 0.15

meV $< \hbar\omega <$ 2 meV. Closely related to this result is the finding by Ramirez *et al.* that the specific heat of SCGO(x) is proportional to T^2 as $T \to 0$. The specific heat data imply that the density of states $\rho(\omega) \propto \omega$. Naively, one might expect that $\chi''(\omega) \propto \rho(\omega)$ for $\omega \to 0$. This is the case for ferromagnets and the few spin glasses where measurements from which these quantities can be derived are available.[10] However, for SCGO(x) this simple relation does not hold. To appreciate what this implies for the ground state of SCGO(x), recall that the response function not only involves the density of states, but also the matrix element of the relevant operator between the ground and excited states. More precisely, at $T = 0$, $\chi''(\omega) \propto \Sigma_j \Sigma_f |\langle f|S_j|0\rangle|^2 \delta(E_f - \hbar\omega)$ whereas $\rho(\omega) = \Sigma_f \delta(E_f - \omega)$. In general we can therefore write $\chi''(\omega) \propto \langle M^2(\omega)\rangle \rho(\omega)$ where $\langle M^2(\omega)\rangle$ can be interpreted as the average squared matrix element of the spin operator at site j, S_j, between the ground state $|0\rangle$ and excited states $|f\rangle$ at energy $E_f = \hbar\omega$. The combination of our data for $\chi''(\omega)$ (Fig. 4) and the specific heat data of Ramirez *et al.*[2,7] Therefore show that $\langle M^2(\hbar\omega)\rangle \propto 1/\omega$ for $\omega \to 0$ in SCGO(x). A more familiar example of an ω-dependent average matrix element is the long-range ordered AFM where it is well established[11] that $\langle M^2(\hbar\omega)\rangle \propto 1/\omega$. Although such behavior is not expected in a system with short-range AFM order only, it may be due to long-range order in a continuous degree of freedom not directly probed by neutron-scattering.

V. TEMPERATURE DEPENDENCE OF THE MAGNETIC FLUCTUATIONS

Apart from the development of weak elastic magnetic scattering, Fig. 4 shows that the freezing transition is preceded and accompanied by modifications in the ω dependence of $\chi''(\omega)$. Note first that the Q width of constant $\hbar\omega$ scans does not increase substantially below 58 K.[12] We can therefore interpret the ω dependence of $\chi''(Q_0,\omega)$ for $T \lesssim 60$ K as that of the local response-function $\chi''(\omega)$. Figure 4 shows that at $T = 58$ K, $\chi''(\omega) \propto \omega$ indicating that a single exponential relaxation process dominates for $\hbar\omega < 2$ meV. At 20 K, $\chi''(\omega)$ deviates beyond error from proportionality with ω, and for $T < 20$ K, it evolves into the low-temperature ω independent form described in IV. To characterize this temperature-dependence further, we have measured $\chi''(\omega)$ at several temperatures and fitted the data to

$$\chi''(\omega) = \chi'(0) \nu \ \mathrm{sign}(\omega) (|\omega|/\omega_c)^{\nu}, \qquad (5)$$

which provides excellent fits at all temperatures investigated. A Kramers–Kronig transformation of (5) within the high-energy cutoff $\hbar\omega_c$ (fixed at 2 meV) shows that $\chi'(0)$ is the real part of the *local* susceptibility corresponding to $\chi''(\omega)$. Figure 5 shows the temperature-dependence of ν and $1/\chi'(0)$ along with that of the elastic scattering at $Q = 1.4$ Å^{-1}. The elastic scattering at high temperatures is incoherent nuclear scattering. Upon cooling there is initially a weak increase which we associate with critical slowing down followed by a sharper approximately linear increase below $T_g = 8$ K. ν decreases gradually from 1 at

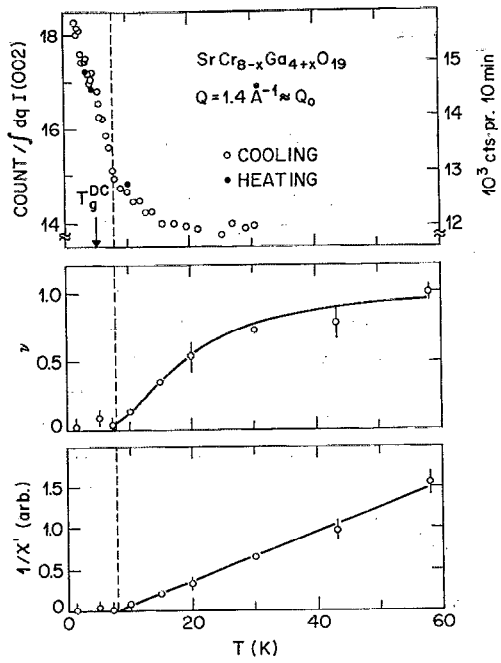

FIG. 5. Temperature dependence of elastic scattering at $Q = 1.4$ Å (configuration No. 1) and the parameters ν and $1/\chi'$ of Eq. (5) which characterize the low energy dependence of $\chi''(\omega)$.

high temperatures and becomes indistinguishable from 0 corresponding to $\chi''(\omega) \propto$ constant below T_g. Not surprisingly, $1/\chi'(0)$ is linear in T at high temperatures and the spin-glass transition is associated with this quantity tending to zero. Note that the temperature $T_g = 8$ K which is indicated by a dashed line in Fig. 5 is larger than $T_g^{dc} = 5$ K derived from susceptibility data.[7] That the temperatures at which anomalies occur depend on the time-scale of the measurement is a well-known property of spin glasses. In summary, not only does a small static moment develop at T_g but the entire low energy part of $\chi''(\omega)$ characterizing the large magnetic fluctuations develops into the anomalous ω independent form at T_g

VI. MONTE-CARLO SIMULATION OF THE AFM KAGOMÉ LATTICE

We have shown that SCGO(x) is a system with many unusual properties, which we suspect are due to the Kagomé lattice structure of the constituent layers. As pointed out in the introduction, there has been exact work[3] on the Ising model on the Kagomé lattice, and some phenomenological descriptions of what might occur for continuous classical spins and low-spin quantum AFMs on Kagomé lattices.[4–6] However, we are unaware of any results which satisfactorily describe the nature of the order (if any) in a classical Heisenberg or xy Kagomé AFM. Thus, before taking on the challenges of quantum mechanics ($S = 3/2$ for Cr^{3+}) and random dilution which are surely relevant for SCGO(x), we consider the classical models on a fully occupied lattice.

The starting Hamiltonian is

$$H=\frac{1}{2}|J|\sum_{(i\neq j)}\mathbf{S}_i\cdot\mathbf{S}_j, \tag{6}$$

where the sum is over pairs of nearest neighbors on the lattice. Unlike the situation for the square lattice, it is impossible simultaneously to minimize the energy for all pairs of neighboring spins. However, it is possible simultaneously to minimize the energies of all triangles of adjacent spins. The latter is accomplished by insisting that the spins at the vertices of each constituent triangle are coplanar and 120° apart. Thus, any ground state of the system can be described as a particular choice at each site from among three spin directions. Thus, once a triad $\mathbf{S}_1$, $\mathbf{S}_2$, $\mathbf{S}_3$ of spin directions has been selected, breaking the continuous symmetry, the Hamiltonian (6) reduces to the three state Potts model, which we have proceeded to study as the simplest departure point for understanding the new physics in SCGO(x). The Hamiltonian is

$$H=\frac{1}{2}|J|\sum_{i\neq j}\delta(n_i,n_j), \tag{7}$$

where δ is the Kronecker delta function. At each site i of the Kagomé lattice, we define a discrete variable n_i which can take on three different values, 1, 2, or 3, corresponding $\mathbf{S}_1$, $\mathbf{S}_2$, or $\mathbf{S}_3$, respectively. For comparison with neutron-scattering data, the quantity of greatest interest is the Fourier-transformed two-spin correlation-function

$$S^{\alpha\beta}(\mathbf{q})=\frac{1}{N}\left\langle\sum_{\mathbf{r}\mathbf{r}'}S^{\alpha}(\mathbf{r})S^{\beta}(\mathbf{r}')\exp[i\mathbf{q}\cdot(\mathbf{r}-\mathbf{r}')]\right\rangle, \tag{8}$$

where $\mathbf{r}$ and $\mathbf{r}'$ are sites in the Kagomé lattice, N is the number of sites, $S^{\alpha}(\mathbf{r})$ is the αth cartesian component of a vector spin at site $\mathbf{r}$ and $\langle\cdots\rangle$ denotes thermodynamic averaging. We relate this expression to the q_p-state Potts model by letting $S^{\alpha}(\mathbf{r})$ take on $q_p = 3$ values S^{α}_n, $n = 1,2,..q_p$ which satisfy $\Sigma_n S^{\alpha}_n = 0$ and $\Sigma_{nn'}\delta_{nn'}S^{\alpha}_n S^{\beta}_{n'} = q_p/2\delta_{\alpha\beta}$. These conditions are clearly satisfied for $q_p = 3$ by three spins separated by 120° in a single plane. Defining $P(\mathbf{r}n,\mathbf{r}'n')$ as the probability that $S^{\alpha}(\mathbf{r}) = S^{\alpha}_n$ and $S^{\alpha}(\mathbf{r}') = S^{\alpha}_{n'}$ the configuration average can be written as

$$S^{\alpha\beta}(\mathbf{q})=\frac{1}{N}\sum_{nn'}\sum_{\mathbf{r}\mathbf{r}'}P(\mathbf{r}n,\mathbf{r}'n')S^{\alpha}_n S^{\beta}_{n'}\exp[i\mathbf{q}\cdot(\mathbf{r}-\mathbf{r}')]. \tag{9}$$

Using the sum-rule $\Sigma_{n'}P(\mathbf{r}n,\mathbf{r}'n') = 1/q_p$ and the Ansatz, based on the symmetry of the underlying Hamiltonian, that for $n'\neq n$ and $n''\neq n$, $P(\mathbf{r}n,\mathbf{r}'n') = P(\mathbf{r}n,\mathbf{r}'n'')$, we can write

$$P(\mathbf{r}n,\mathbf{r}'n')=\frac{1}{q_p}\left(\delta_{nn'}P_{eq}(\mathbf{r},\mathbf{r}')+(1-\delta_{nn'})\frac{1-P_{eq}(\mathbf{r},\mathbf{r}')}{q_p-1}\right), \tag{10}$$

where $P_{eq}(\mathbf{r},\mathbf{r}')$ is the probability that sites $\mathbf{r}$ and $\mathbf{r}'$ are in the same spin state. Inserting (10) in (9) we obtain

$$S^{\alpha\beta}(\mathbf{q})=\frac{1}{2}\delta_{\alpha\beta}\left(1+\frac{1}{N}\sum_{\mathbf{r}\neq\mathbf{r}'}\frac{q_pP_{eq}(\mathbf{r},\mathbf{r}')-1}{q_p-1}\times\exp[i\mathbf{q}(\mathbf{r}-\mathbf{r}')]\right). \tag{11}$$

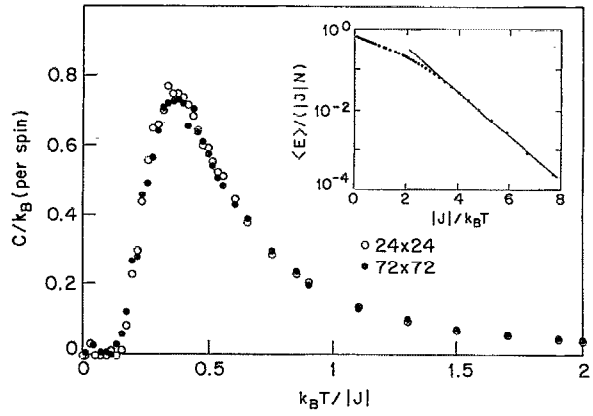

FIG. 6. Specific heat vs temperature for the three states Potts model on the Kagomé lattice determined by Monte-Carlo simulation on a 24×24 (○) and 72×72 (●) lattice. Insert shows internal energy vs inverse temperature.

We determined $P_{eq}(\mathbf{r},\mathbf{r}')$ from $T\approx 0$ states generated by gradual cooling of randomly generated high-temperature states by the Metropolis technique.[13] To speed convergence to thermal equilibrium, especially at low temperatures, single spin-flips and rotations of clusters of six spins forming hexagons [Fig. 1(b)] were attempted in alternation. During cooling we measured the energy $\langle E\rangle/(|J|N)$ defined by (6), the specific heat per spin $C(T)/k_B = (\langle E^2\rangle - \langle E\rangle^2)/(Nk_B^2T^2)$, and the average number of hexagons with a Potts-state sequence nn' nn' nn'. Starting from the equilibrium state at the previous temperature, a sequence of states was generated by attempting to flip each spin and rotate each hexagon in the lattice. Equilibrium at each temperature was declared when none of these quantities determined by averaging over $K/2$ states differed more than $R\%$ (typically 1%–5%) from the average obtained from the next K states. The latter averages were then recorded as the thermal equilibrium values and R as the relative error. Lattices from 24×24 to 72×72 were studied with periodic boundary conditions and typically K varied between 4096 and 32768.

VII. SPECIFIC HEAT

Figure 6 shows the $C(T)$ for a 24×24 and a 72×72 lattice. There is a broad peak centered around $k_BT/|J| = 0.4$. Since the results for lattices with linear dimensions differing by a factor of 3 coincide, we conclude that the results for the 72×72 lattice are representative for the infinite lattice. Since most of the entropy is removed in a broad specific-heat peak, not by a phase-transition. Figure 6 indicates that the AFM three-state Potts model does not have a finite-temperature phase-transition on the Kagomé lattice. The insert shows $\langle E\rangle/(|J|N)$ in a logarithmic plot demonstrating that for $T\to 0$, $\langle E\rangle/(|J|N)$ is exponentially activated, as must be the case for any system with a discrete local symmetry. The activation energy, $E_a = 1.3 \pm 0.1|J|$ for the 72×72 lattice. An upper bound on E_a is

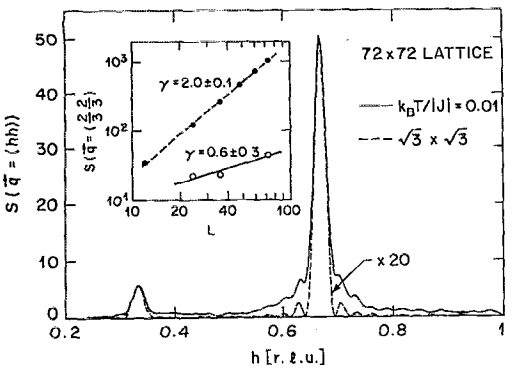

FIG. 7. Monte-Carlo data for $S(\mathbf{q})$ on a 72×72 lattice along the (hh) direction at $k_BT/|J| = 0.01$ (solid line) and for the corresponding LRO state on the same lattice (dashed line which is reduced by a factor of 20). Insert shows $S(\mathbf{q}_{\rm tri})$ vs lattice size for the same states.

the energy, $2|J|$ required to flip a single spin at $T = 0$. The lower value of E_a results from correlations between spin flips.

VIII. STATIC CORRELATION FUNCTION

The static correlation function in the state obtained by the cooling sequence of Fig. 6, $S^{\alpha\beta}(\mathbf{q})$ was calculated from (11). We determined $P_{eq}(\mathbf{r},\mathbf{r}')$ in an irreducible zone compatible with the local symmetry by averaging over each site the probability of an equal spin at each other site in the lattice. To improve statistics, averaging was also performed over 5 lattices obtained by random rotation of symmetric hexagons in the low-temperature state. Figure 7 shows $S^{\alpha\alpha}(\mathbf{q})$ for the 72×72 lattice. The momentum $\mathbf{q}$ is indexed in the hexagonal reciprocal lattice $a^* = b^* = 4\pi/\sqrt{3}a$, $\gamma = 60°$, a being the Kagomé lattice parameter. There are sharp peaks at $\mathbf{q}_{\rm tri} = (\frac{2}{3}\frac{2}{3})$ indicating that antiferromagnetic order corresponding to the periodic tripartition of the Kagomé lattice occurs with a substantial correlation length. For comparison, the dashed line shows $S^{\alpha\alpha}(\mathbf{q})$ for the long-range ordered (LRO) state. The width of this peak is due to the finite size of the 72×72 lattice. The relative intensity of the $(\frac{2}{3}\frac{2}{3})$ and $(\frac{1}{3}\frac{1}{3})$ peaks are the same for the two states, indicating that the AFM structure is similar. However, the mean square staggered magnetization $S^{\alpha\alpha}[\frac{2}{3},\frac{2}{3}]$ of the gradually cooled state is 20 times less than that corresponding to LRO, indicating substantial disorder, as anticipated due to the large ground-state degeneracy. Furthermore, although the FWHM of the peaks for the two states is similar, the peaks of the gradually cooled state have substantial tails. These observations are consistent with the presence of algebraically decaying correlations. Another indication of this comes from the lattice size dependence of $S^{\alpha\alpha}[\frac{2}{3},\frac{2}{3}]$ shown in the inset. For correlations decaying according to $|r|^{-\eta}$ and for sufficiently large $L\times L(=N)$ lattices $S^{\alpha\alpha}(\mathbf{q}_{\rm tri}) \propto L^{\gamma}$, where $\gamma = d - \eta$, $d = 2$ being the lattice dimensionality.[13] For the long-range ordered state, $\gamma = 2.0\pm0.1$ as anticipated, whereas $\gamma = 0.6\pm0.3$ corresponding to $\eta = 1.4\pm0.3$ for the state obtained by gradual cooling.

IX. SUMMARY AND CONCLUSIONS

We have shown that despite strong AFM interactions, SCGO(x) has a strongly fluctuating and short-range ordered ground-state. The two-dimensionality and wave vector $\mathbf{q}_{\rm tri}$ of the order confirms the conjecture by Ramirez *et al.*[2] that magnetic frustration on the Kagomé lattice is the origin of this anomalous ground-state. Monte Carlo simulation of the three-state Potts model on the Kagomé lattice show that the model is critical at $T = 0$ with algebraic correlations of the staggered magnetization at $\mathbf{q} = \mathbf{q}_{\rm tri}$. Comparison with the experimental system suggests that for $S = \frac{3}{2}$ Heisenberg spins, quantum fluctuations, which are strong in our experiment, destroy even the algebraically decaying two-spin correlations. Even so, an interesting property of AFMs with long-range order remains, namely a $\frac{1}{\omega}$ divergence of the overlap $\langle M^2(\omega)\rangle$ between the groundstate with a single spin-flip and the excited states. Whether this is a characteristic property of geometrically frustrated quantum AFMs remains to be seen.

ACKNOWLEDGMENTS

We thank A. P. Ramirez for sharing his data with us and for stimulating discussions, and D. Huse for discussions and tutoring in the Monte Carlo technique. We are also grateful for the hospitality and assistance of the staff of Risø National Laboratory during the experiment.

[1] X. Obradors, A. Labarta, A. Isalgue', J. Tejada, J. Rodriguez, and M. Pernet, Solid State Commun. **65**, 189 (1988).
[2] A. P. Ramirez, G. P. Espinosa, and A. S. Cooper, Phys. Rev. Lett. **64**, 2070 (1990).
[3] I. Syozi, in *Phase Transitions and Critical Phenomena*, Vol. 1, edited by C. Domb and M. S. Green (1972), p. 269; R. Liebmann, *Statistical Mechanics of Periodic Frustrated Ising Systems* (Springer, New York, 1986), and references therein.
[4] V. Elser, Phys. Rev. Lett. **62**, 2405 (1989).
[5] I. Ritchey and P. Coleman, Bull. Am. Phys. Soc. **35**, 800 (1990).
[6] P. Chandra and P. Coleman, Rutgers University Report No. 90-18 (to be published).
[7] A. P. Ramirez, G. P. Espinosa, and A. S. Cooper, preprint (1990).
[8] C. Broholm, G. Aeppli, G. P. Espinosa, and A. S. Cooper, Phys. Rev. Lett. **65**, 3173 (1990).
[9] This is strictly correct only when Q is far outside the first Brillouin zone. However, it is a good approximation for smaller Q when the correlation length is short.
[10] D. Mechede, F. Steglich, W. Felsch, H. Maletta, and W. Zinn, Phys. Rev. Lett. **44**, 102 (1980); L. E. Wenger and P. H. Keesom, Phys. Rev. B **13**, 4053 (1976); C. C. Paulsen, S. J. Williamson, and H. Maletta, Phys. Rev. Lett. **59**, 128 (1987).
[11] G. Aeppli *et al.*, Phys. Rev. Lett. **62**, 2052 (1989).
[12] G. Aeppli, C. Broholm, and A. P. Ramirez (unpublished).
[13] K. Binder and D. W. Hermann, *Monte Carlo Simulation in Statistical Physics* (Springer, New York, 1988).